Survey of Selected Additively Manufactured Propellants for Arc-Ignition of Hybrid Rockets

Stephen A. Whitmore,[1] Stephen L. Merkley[2], Louis Tonc[3], and Spencer D. Mathias[4]

Utah State University, Logan Utah, 84322-4130

Results of a testing campaign to assess multiple commercially available 3-D printer materials for effectiveness in an arc-ignition system for hybrid rockets are presented. Previously, a form of additive manufacturing known as Fused Deposition Modeling was used to fabricate high-density acrylonitrile butadiene styrene fuel grains so that, when properly layered possess unique electrical breakdown properties. When subjected to an inductive charge an electrical-arc flows along the layered material surface and "seeds" combustion when the arc occurs simultaneously with the introduction of an oxidizing flow. This study investigates commercially available 3-D printable materials to search for equivalent or possibly superior fuel alternatives to ABS. Test specimens include photopolymers processed using polyjet (stereo-lithography) and fused-deposition printing. Comparison metrics include general arc-ability, pyrolysis rate, dissipated power, characteristic velocity, and ability for multiple restarts. Initially, an ensemble of 8 commonly-available "printable" polymers was evaluated, and only 4 printable materials -- high- and low-density ABS, VeroClear®, and white polycarbonate -- were found to possess effective "sparking" properties. In follow-on burn tests only high- and low-density ABS and VeroClear performed effectively as fuel materials. White polycarbonate would not ignite using the arc-method. High-density ABS exhibited the best overall ignition properties and characteristic velocity.

[1] Professor, Mechanical and Aerospace Engineering Department, 4130 Old Main Hill, UMC 4130, Associate Fellow, AIAA.
[2] Graduate Research Associate, Mechanical and Aerospace Engineering Department, 4130 Old Main Hill, UMC 4130, Student Member, AIAA.
[3] Graduate Research Associate, Mechanical and Aerospace Engineering Department, 4130 Old Main Hill, UMC 4130, Student Member, AIAA.
[4] Undergraduate Research Assistant, Mechanical and Aerospace Engineering Department, 4130 Old Main Hill, UMC 4130, Student Member, AIAA.

Nomenclature

CEA	=	Chemical Equilibrium with Applications (computer program)
c^*	=	characteristic velocity, *m/sec*
$c^*_{measured}$	=	measured characteristic velocity, *m/sec*.
$\dot{E}$	=	power required to pyrolize material, *J/sec*
h_v	=	enthalpy of gasification, *MJ/kg*
I	=	high voltage power supply output current, *mA*
$\dot{m}$	=	massflow of pyrolysis products, *g/sec*
$\dot{m}_{ox}$	=	oxidizer massflow, *g/sec*
$\dot{m}_{nozzle}$	=	total motor exit massflow, *g/sec*
O/F	=	oxidizer to fuel ratio
$P_{dissipated}$	=	dissipated power, *J/sec*
P_0	=	chamber pressure, *kPa*
p	=	pressure of pyrolized fuel vapor, *kPa*
R_g	=	gas constant of pyrolysis products, *J/kg-K*
T	=	temperature of pyrolized gas, *K*
V	=	high voltage power supply output potential, *V*
Vol	=	chamber volume, cm^3
η^*	=	combustion efficiency, c^*_{meas}/c^*_{ideal}
ρ	=	density, g/cm^3
$\dot{\rho}$	=	rate of change of density c, $g/sec\text{-}cm^3$

I. Introduction

Because hybrid rocket propellant materials are individually chemically stable prior to mixing within the combustion chamber, these systems possess well-known safety advantages. Unfortunately, the relative stability of traditional hybrid propellants also makes hybrid systems difficult to ignite. Hybrid rockets have traditionally used

large, high output pyrotechnic or “squib” charges to initiate combustion. Pyrotechnic ignitors are capable of producing very high-enthalpy outputs, but are extremely susceptible to the *Hazards of Electromagnetic Radiation to Ordnance* (HERO) [1], and the pyrotechnic charges associated with large single-use ignitors charges present a significant operations hazard. Most importantly, for nearly all applications pyrotechnic ignitors are designed as "one-shot" devices that do not allow a multiple restart capability. Thus, the great potential for multiple re-start upper stages using hybrid rockets remains largely unrealized.

II. Background on Ignition Technologies

Several existing technologies have been investigated to overcome the ignitibility shortcomings described in the previous paragraph. These methods include 1) plasma torch, 2) electric spark plugs with bi-propellant oxidizer and fuel injectors, 3) pyrophoric ignition fluids, 4) ignition featuring hypergolic bi-propellants, and 5) catalytic dissociation of one or more of the hybrid propellants. All of these methods possess distinct disadvantages that make application to hybrid rocket systems impractical.

A. Conventional Ignition Technologies.

Plasma torches are devices for generating a directed flow of plasma, and have been effectively used for gas turbine engines and supersonic combustion ramjets for ground test articles. [2] These devices produce very high output temperatures, but have a low total mass flow. Achieving a high-total output enthalpy requires a large input power. Typically, the power production units (PPU) for these devices are heavy and not generally amenable to flight applications except an initial launch vehicle stage where the ignition power can be provided by a ground based PPU.

Clearly, bi-propellant ignitors are capable of producing sufficient enthalpy to act as ignition sources for hybrid propellants; however, the complexity required by the dual-propellant feed path, and potential combustion stability issues present significant operational disadvantages. Bi-propellant ignitors are difficult to properly tune, and immediate ignition as the propellants enter the combustion chamber is essential to avoid "hard starts." Ignitor flame holding stability is also a critical issue.

Pyrophoric ignition liquids fluids like Triethylaluminum-Triethylborane (TEA-TEB), and monopropellants like hydrazine are highly reliable, produce high output enthalpies, and can be used for multiple re-starts. [3] Unfortunately, like hydrazine, this class of hazardous propellants presents the extreme disadvantage of being highly

toxic, potentially explosive, and expensive to work with during ground processing. The use of pyrophorics defeats the advantages of using safe and non-toxic hybrid propellants.

Like pyrophorics, hypergolic propellants allow for a consistent and reliable ignition enthalpy source, and have been used for multiple space propulsion systems. [4] Unfortunately, hypergolic bi-propellant ignition systems feature both an operations hazard, in addition to the feed-system complexity of a bi-propellant system. To date, a hypergolic ignition system has never been seriously considered for a hybrid rocket.

Finally, multiple researchers have investigated the catalytic decomposition of nitrous oxide (N_2O) to initiate hybrid rocket combustion. [5], [6], [7] Unfortunately, in all cases the decomposition bi-products were so hot that all existing catalyst bed materials were consumed after one or two ignitions. Thus, multiple restart capability has not been demonstrated. Also, to ensure reliable ignition N_2O cat beds must be pre-heated greater than $350\ ^oC$ before ignition. This pre-heat requires a considerable power source and is not compatible with small "rideshare" spacecraft where hybrid systems show a competitive advantage.

B. Arc-Ignition of Additively-Manufactured Acrylonitrile Butadiene Styrene (ABS).

While characterizing the performance of additively-manufactured ABS as a replacement for conventional hybrid rocket fuels, [8] it was discovered that the layered material structure of additively-manufactured ABS, fabricated using a type of additive manufacturing known as fused deposition modeling (FDM) [9], concentrates minute electrical charges that produce localized arcing between material layers. Joule heating -- the process by which the passage of an electric current through a conductor releases heat -- from the resulting arc produces a small but highly-conductive melt layer. This melt layer allows for very strong surface arcing to occur at moderate input voltage levels -- between 200 and 300 volts. Additional Joule heating from the strong surface arcing causes a sufficient fuel material to vaporize, seeding combustion when simultaneously combined with an oxidizing flow.

The discovery of FDM-processed ABS' unique electrical breakdown characteristics prompted the invention of an ignition system that takes advantage of the previously described "hydrocarbon seeding" phenomenon. [10], [11] Figure 1 illustrates the top-level concept, where two electrodes are embedded within an ABS fuel grain segment. The conducting paths terminate in electrodes that are flush with the combustion port surface and exposed to the interior of the combustion chamber. The layered structure of the FDM-processed ABS provides local surface features of very small radius. As a voltage is applied across the two electrodes, these surface features serve to

concentrate charge at many discrete points the material surface. The effect produces a large ensemble of "electrodes" with a gap- distance on the order of microns. These features allow electrical breakdown -- and thus electrical arcing -- to occur at moderate voltage levels. For properly designed system geometry the separation distance, and thus the breakdown voltage between the metal electrodes is too high to initiate direct metal-to-metal arcing; rather arcing occurs along the surface of the ABS fuel. The image on the left-hand side of Figure 1 shows the inductive spark propagating along the grain surface, and the schematic on the left hand side shows the resulting fuel pyrolysis.

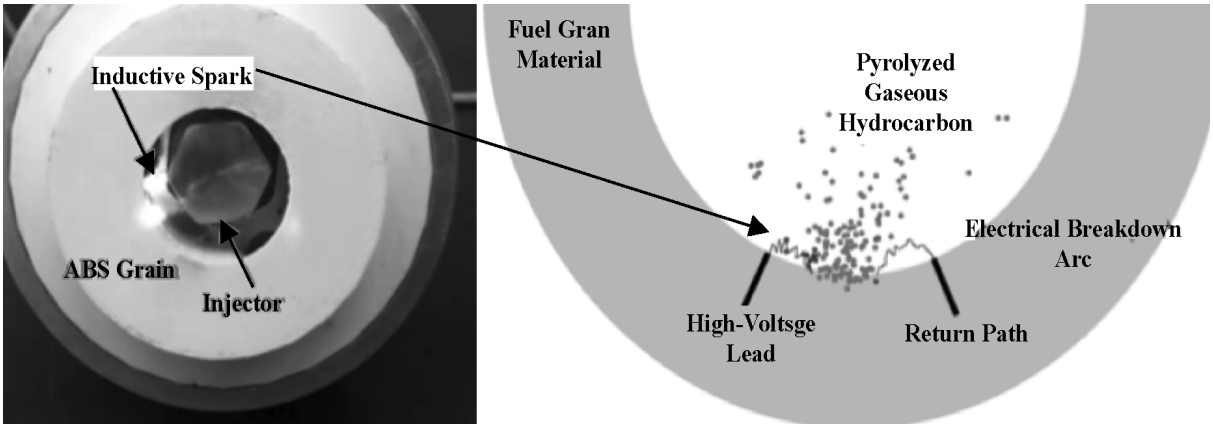

Figure 1: Arc Ignitor with Joule-Heating Concept Demonstration.

During this initial phase of testing, the authors discovered that particular orientation of the FDM-processed material layers had a significant effect on the arcing process. In order to qualitatively assess this effect, three conical grains were manufactured; two grains using a Stratasys Dimension® 3-D *FDM* printer, and the other grain machined from extruded ABS stock material. One FDM-processed ignitor grain was printed "vertically-stacked," that is, with deposition layers parallel to the longitudinal axis of the motor and direction of oxidizer flow. The second grain was printed "horizontally-stacked," with deposition layers perpendicular to the longitudinal axis of the motor and perpendicular to the direction of oxidizer flow.

After several arc-breakdown cycles, the vertically-stacked ignitor grain ceased to visibly arc. In order evaluate this result, the grain was cut along the longitudinal axis and inspected. Patterns of heavy char indicated that an alternate path between the electrodes had formed, and any circuit closure was occurring internal to the grain surface. Because the loop was closed internal to the grain surface, fuel pyrolysis and the resulting vapor generation did not

occur. This behavior was observed for several vertically-stacked test specimens. This behavior did not occur in any of the horizontally-stacked specimens tested, and indicates that horizontal-stacking is the preferred method of manufacture.

C. Arc-Ignition Prototype Development.

The discovery of ABS' unique electrical breakdown characteristics prompted the invention of prototype hybrid ignition system that takes advantage of the previously described electrostatic breakdown phenomenon. Because the primary objective of this test campaign was to optimize the arc-ignitor fuel grain design, it was deemed too costly and time consuming to manufacture multiple full-scale 98 mm hybrid fuel grains; thus, as a lowered-cost alternative an existing 98-mm motor cap previously used for hybrid motor testing was adapted to fit into a short 10.2 cm hybrid motor section. Figure 2 shows an exploded view of this developmental unit, dubbed as *"Little Joe."* The design was engineered such that nozzle geometries could be quickly varied to provide a range of internal chamber pressure conditions. The oxidizer for these tests was gaseous oxygen (GOX). The GOX injector feed pressure was adjusted using a manual pressure-reducing regulator. The pictured configuration shows a water-cooling jacket, which was deemed unnecessary after the initial series of tests and removed for subsequent testing.

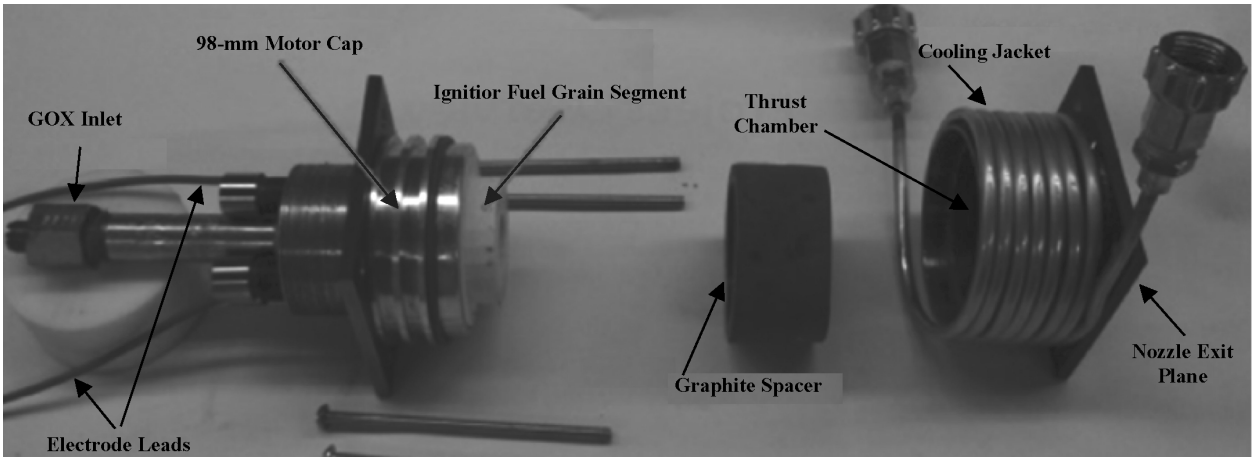

Figure 2. Exploded View of the "Little Joe" Ignitor System Development Motor.

Three different ignitor-grain geometries were evaluated during the "Little Joe" development tests. These configurations were 1) a conical converging section, 2) a stepped-cylindrical section with a flow impingement "shelf," and 3) a stepped-cylindrical section with dual impingement shelves. The first two geometries employed a straight single port injector and the final dual-shelf geometry was tested using coaxial injector with an axial port, and

two side injection ports. During this testing campaign only configuration 3 performed in a reliable and effective manner, and this configuration was adapted as a baseline for follow-on testing. This novel, low-power arc-ignition technology overcomes many of the previously-described issues associated with conventional technology ignition methods.

D. Arc-Ignition Testing with Embedded Fuel Grain Ignitor.

In order to demonstrate a "drop-in" application of the developed technology, the testing campaign of Ref. [10] concluded with a series of tests that embedded the developed ignitor system into the top end of a lab scale 75-mm hybrid rocket motor. This well-characterized motor system had been previously tested at Utah State, but with ignition being initiated by a set of single-shot pyrotechnic charges. [12] Figure 3 shows the FDM-fabricated fuel grain with the integrated ignitor section. The design takes advantage of FDM-processing to build the ABS ignitor and fuel grain sections with "snap-together" interlocks that allow individual grain segments to be manufactured separately, and then assembled for combustion. The embedded electrodes fit into slots manufactured in the motor injector cap. Figure 4 shows a schematic of the integrated motor case. As shown in this figure the initial fuel grain port was manufactured with a helical structure in order to increase regression rate and combustion efficiency. [13]

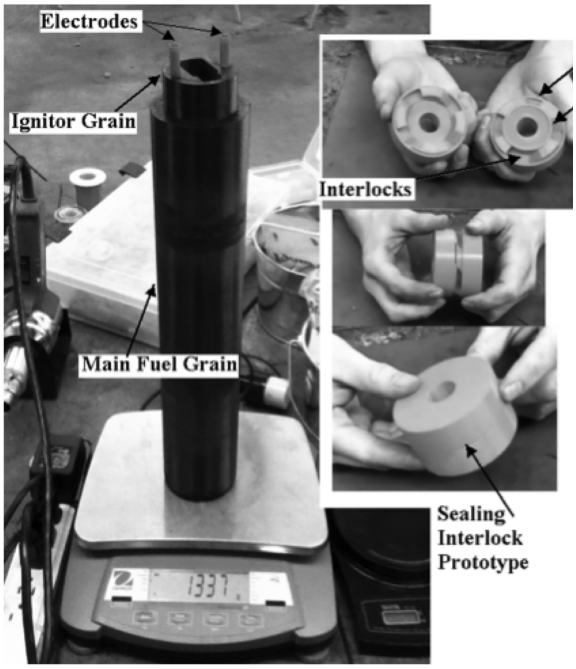

Figure 3. FDM-Fabricated ABS Fuel Grain with Integral Ignitor and Interlocking Fuel Grain

The developed system allowed for multiple consecutive “hands off" re-starts of the 75 mm motor with the embedded ignitor grain. The burn profiles exhibited excellent run-to-run consistency with low deviations in both thrust and chamber pressure. Also the response fidelity of the integrated arc-ignition system was consistently greater than occurred using conventional 1-shot pyrotechnic ignitors on the same system, indicating that the additional chamber volume downstream of the ignitor section has little effect upon the ignition kinetics.

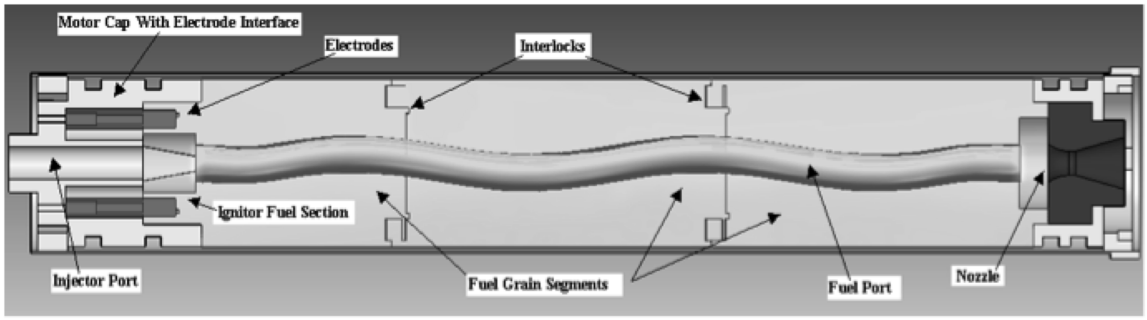

Figure 4. Schematic of 75-mm Motor Case with Integrated Arc-Ignitor.

For these tests, the motor featured a semi-optimized nozzle with an expansion ratio of 3.5. The mean delivered I_{sp} at ambient conditions was 228.7 seconds at a combustion chamber pressure of 1380 kPa (psia). This delivered specific impulse extrapolates to a vacuum I_{sp} of greater than 300 seconds using a 20:1 expansion ratio nozzle -- significantly higher than can be achieved by a hydrazine-based system. Both the ignitor and fuel sections for this design were fabricated using the commercially available ABSplus-P340® [14] feed-stock material.

III. Propellant Testing with Alternative Additively Manufactured Materials.

Shortly after the initial discovery, the authors of Ref. [10] made several unsuccessful attempts to reproduce a similar phenomenon with other hybrid fuel materials including Hydroxyl Terminated Polybutadiene (HTPB), acrylic, paraffin, and extruded ABS. These specimens were fabricated using traditional methods, with the HTPB and paraffin test articles being cast using molds, and the acrylic and ABS extruded specimens being manufactured using conventional machining. The cast and machined materials, even though possessing identical geometries to the FDM-processed specimens, were completely ineffective. Thus, the authors have concluded additive-manufacturing is a key element to achieving the previously described advantageous arcing properties.

A. Summary of Test Materials.

This section summarizes follow-on testing campaign, where multiple 3-D printable materials were evaluated for suitability as the fuel component for hybrid rocket systems that employ the previously described arc-ignition system. This study investigates materials and manufacturing processes to search for equivalent or possibly superior alternatives to the ABSplus FDM-feedstock material previously evaluated during the prototype testing campaign. Table 1 shows the list of candidate materials to be evaluated. The study did not attempt to design or optimize the

plastic materials, but instead simply evaluated the effectiveness of common commercially-available 3-D printer materials[10].

Test Specimens fabricated with both PolyJet (photopolymers) and FDM (thermoplastic) techniques were investigated. PolyJet technology is a lithographic additive manufacturing method that is traditionally used to build smooth, accurate prototypes, parts, and tooling. With 16-micron layer resolution and accuracy as high as 0.1 mm, PolyJet can produce thin walls and complex geometries using the widest range of materials. PolyJet 3D printing is similar to inkjet printing, but instead of jetting drops of ink onto paper, PolyJet 3D printers jet layers of curable liquid photopolymer onto a build tray. The built layers are cured using ultraviolet light. Fused Deposition Modeling (FDM) is an additive manufacturing method where a plastic filament is unwound from a coil and supplies material to an extrusion nozzle. The extruded material cools and sets once contacted with the built model. Depending on the model complexity, FDM objects may be built with or without a support structure that must be dissolved away once the part is complete.

Table 1. Properties of Additive-Manufactured Materials Evaluated for Ignition Testing

		Photopolymers						**Thermoplastic**		
Material Name		VeroClear	Durus-white	RGD 720	Digital ABS	Tango-Plus	EBS-ED7	FDM Poly-Carbonate	PC-ABS Blend	ABS-Plus P340
Property		Rigid	Semi-Flexible	Rigid	ABS-Like (RGD515/ RDG535 Blend)	Flexible Rubber-like	Static Dissipative	High Strength	High Impact	Most Common
Color		Transparent	White	Semi-clear	Green	Black	Black	White	Black	Multiple
Tensile Strength	ksi	7-9	2.9-4.35	7.25-9.45	8.8-8.7	1.15-2.2	5.2	9.8	5.9	4.7
Tensile Elongation	%	10-25%	40-50%	15-25%	25-40%	170-220%	4%	4.8%	6%	6%
Flexural Strength	Mpa	75-110	30-40	80-110	65-75	61	104	68	196	55
IZOD Impact	J/m	20-30	40-50		20-30	1.2-1.5		111	53	196
Heat	De	113-122	99-108	113-122	136-154	N/A	204	271	230	204

[10] Anon., Stratasys, "Materials, Explore the widest range of materials in the 3D printing world," http://www.stratasys.com/materials, [Retrieved 15 Nov. 2015].

Deflection Temperature @ 66 psi	g F.

1. *PolyJet (Photopolymer) Materials* [16]

In the above table the PolyJet material VeroClear® is a rigid, nearly colorless photopolymer featuring proven dimensional stability for general purpose, fine-detail prototypes. Duruswhite® is a milky-white simulated polypropylene material that is created for high strength and elongation resistance. RGD720® is a rigid semi-clear plastic acrylic-based photopolymer material with a yellowish tint. Digital ABS® is greenish polyjet material fabricated from blended Stratasys Inc.'s proprietary RGD515 and RGD535 polymers. Digital ABS is a photopolymer designed to simulate ABS engineering plastics by combining high-temperature resistances with high toughness. Tango-plus is a soft-flexible, simulated rubber, PolyJet material with a dark black coloring.

2. *FDM (Thermoplastic) Materials* [17]

In additional to conventional part built from ABSplus feed stock, ABS-ESD7 [18] was also investigated. This material stock has embedded non-carbon alloys, carbon powder, and carbon fibers, added to increase the conductivity as a measure to control static electricity formation in encapsulated electronics. Typical impedances are 5-10,000 Ω/cm. Some properties of the original ABS material are modified by the addition of the filler materials; but chemical resistance, strength, and manufacturability remain generally the same. The last two alternative materials investigated include a white polycarbonate material designed for high strength, and a polycarbonate PC-ABS blend designed for high impact resistance. For the pyrolysis and hot-fire tests, the alternative specimens were compared against ABSplus grains manufactured at high density (975 g/cm^3) and with a 50% reduction in print density (485 g/cm^3).

3. Test Specimen Form Factor

Figure 5 shows the fuel grain form factors that were evaluated. In this design, the ignitor grain segment was manufactured with empty electrode paths incorporated into the structure. After the fuel-segment was manufactured and cured, the arc-ignition electrodes were manually inserted into the electrode paths. The electrode slots were then "capped" with additively-printed ABS filler material, and bonded with plastic cement. As pictured, the grain shows the non-conductive elements with the electrodes that are later bonded into the top of the ignitor grain segment. This design reproduces the most successful ignitor and electrode interface geometry of Ref. [11]. As a cost saving

measure, the test specimens were manufactured to be only 60% of the length of the ABS test specimens previously tested by Ref. [11].

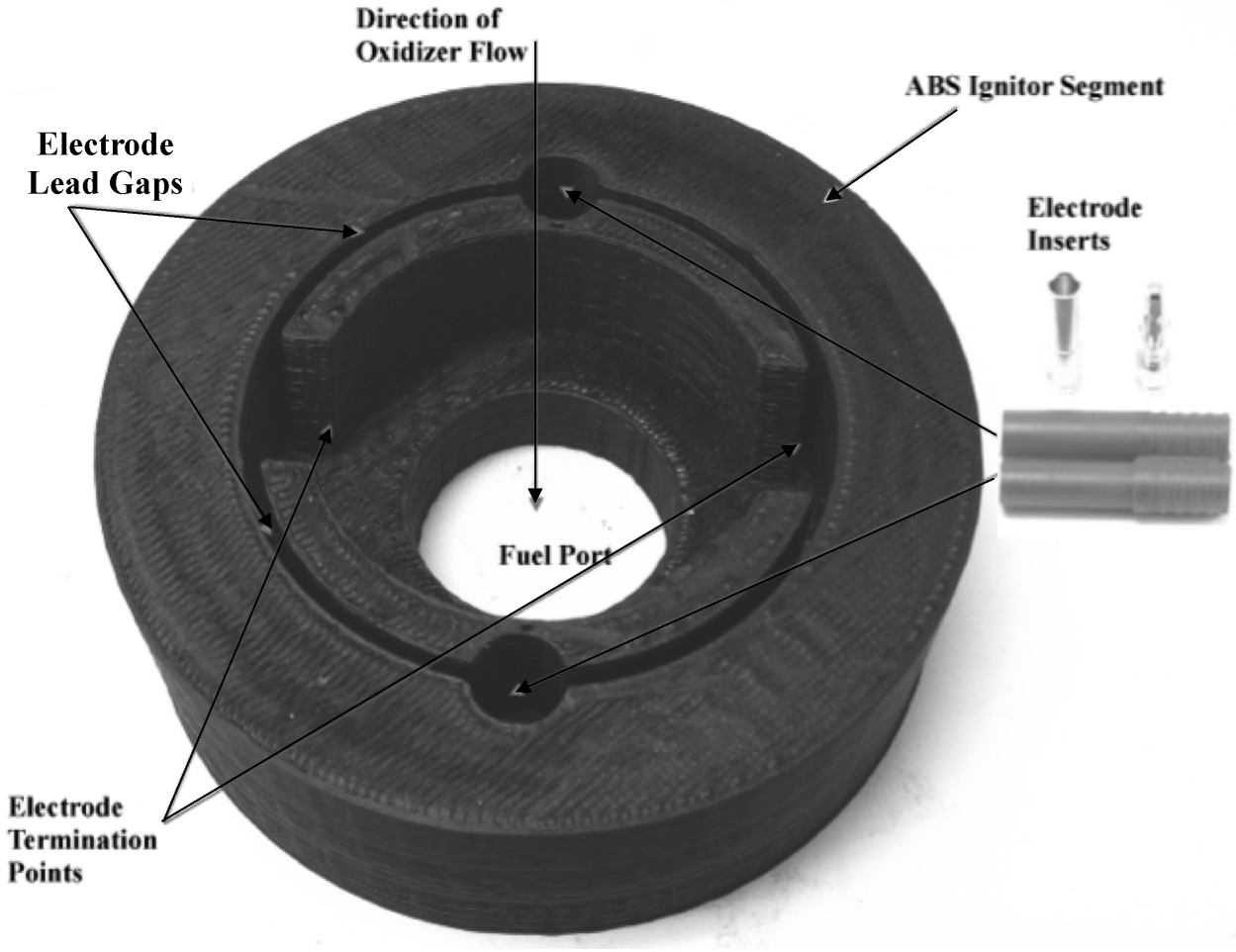

Figure 5. Dual-Material Grain Element with Printed Electrode Paths.

B. Test Results.

This section details the tests that were performed in order to evaluate the suitability of the various plastic materials as arc-ignitable hybrid rocket fuels. Each of the materials of Table 1 was tested for minimum spark capability. For each material that could be "sparked" using a reasonable voltage and current level, a series of follow-on pyrolysis tests were performed to evaluate the rate of hydrocarbon gas generation and required power input levels. Finally, any of the "surviving" fuel materials were burned as fuel in a small hybrid rocket demonstrator.

4. "Spark" Tests

Initial tests during this testing campaign examined the basic "sparkability" of each of the 8 printed materials listed in Table 1. High and low-density, horizontally-layered ABS specimens were used as control measures. For these tests precision two types high voltage power supply (HVPS) manufactured by UltraVolt, Inc. [19] were used to supply the input power. Both 6- and 30-watt units were tested. The higher-voltage 30-Watt unit -- current-limited at *14.5 mAmps* -- was used to "set" the fuel grain, and then the lower power unit -- current limited at *6 mAmps* -- was used as the power source for follow-on pyrolysis and burn testing.

With a freshly manufactured grain the material impedance is very high, and the arc generally jumps the air gap between the electrodes. Coating the desired arc path with carbon black and arcing initially sets the fuel material. This action provided a positive path along the material for the spark, and helped to initiate joule heating and pyrolysis of the fuel materials. Once the grain material is "set," sufficient fuel material has been pyrolyzed to form a slightly conductive char-path along the material surface. This conductive path still possesses impedances typically greater than 10 kΩ; but lower than the air-gap impedance. Figure 6 shows a typical "set" and "unset" ABS grain spark behavior during the initial grain conditioning process.

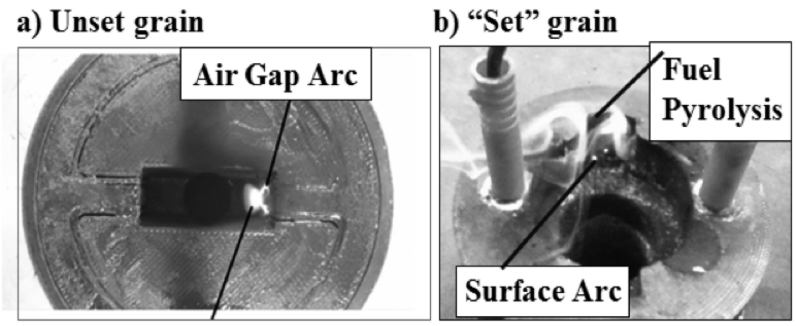

Figure 6. Arc-Path Properties for Unset and "Set" Fuel Grains.

In addition to the two high- and low-density ABSplus-470 grain segments, only one of the photopolymers, *VeroClear,* and one of the thermoplastic materials, *white polycarbonate,* (*WPC*) exhibited sustained sparking properties. Thus, only 4 fuel materials, 1) high-density, 2) low-density FDM-printed ABS, 3) FDM-printed polycarbonate, and 4) VeroClear printed using PolyJet, were carried forward for pyrolysis testing. For the other materials, once the seeding graphite burned away the spark either resumed arcing across the air gap-- *Duruswhite, Digital ABS, Tango Plus*, or buried into the material -- *ABS ESD7, Polycarbonate-ABS blend*, resulting in no external hydrocarbon vapor for seeding combustion.

Figure 7 shows a typical combustion behavior for the ineffective fuel materials -- in this case the ABS ESD7 specimen. Figure 7a plots the internal chamber pressure produced by pyrolysis fuel material, and Fig 7b plots the dissipated electrostatic power. Here, for the first 4 seconds of the initial test the specimen produces significant fuel pyrolysis and the dissipated power exceeds 2 watts. For subsequent tests no spark was observed and the fuel pyrolysis rate drops to zero. Once the seeding carbon black on the surface has burned away leaving only the native material behind, the connection between the electrodes essentially becomes an open circuit.

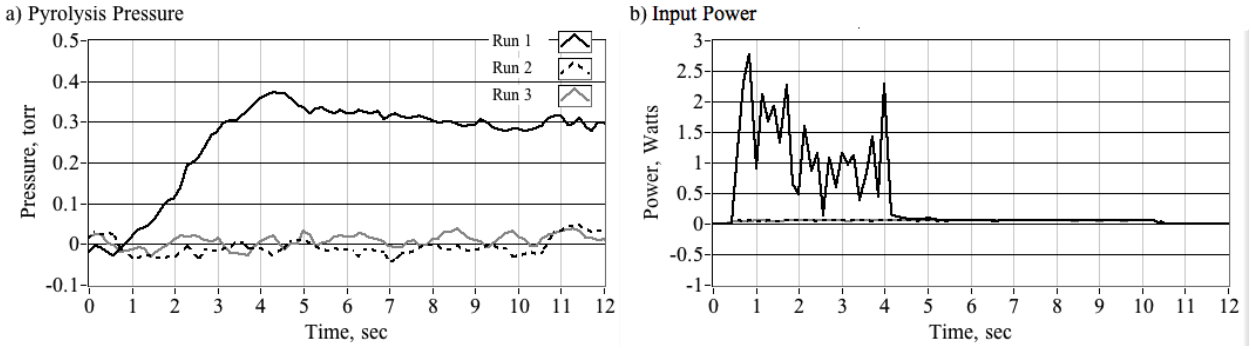

Figure 7. Fuel Pyrolysis Behavior of Graphite-Seeded ABS ESD7.

5. Initial Arc-Pyrolysis Tests

This series of pyrolysis tests evaluated rate of hydrocarbon gas generation and required power input levels when the test specimen is subjected to an inductive spark in a closed chamber. The primary objective of this series of tests was to measure the relative rates of fuel pyrolysis for a given input power level. In this test setup, a shortened version of the original "Little Joe" apparatus was employed and a sealing plate covered the nozzle exit. The injector inlet was capped and the original 500-psig pressure transducer was replaced with a high sensitivity $\pm$0.75 psi differential pressure transducer. A small hand-operated vacuum pump was connected to the injector inlet, replacing the oxidizer feed line. Once the test cylinder was sealed, the hand-held vacuum pump was used to mostly evacuate the chamber and the 6-watt HVPS was used to spark the grain for a prescribed time period – typically 10 seconds. The resulting pressure rise was recorded. The input current and voltage produced by the HVPS was also recorded to allow calculation of the power dissipated by the fuel specimen.

Figures 8, 9, 10, and 11 compare typical time history traces of the resulting pyrolysis pressure and input power for the pyrolysis tests of the *High- and Low-density ABS, VeroClear, and WPC specimens.* In these trials each of the 4-most effective test materials were tested 5 times to measure the rate of materials pyrolysis and consumed input

power. Both the High- and Low-density ABS specimens exhibit similar behaviors, with the exception that the low-density material shows a slightly higher pyrolysis rate. The pyrolysis pressures of the low-density ABS and VeroClear are comparable; however, the power consumed in pyrolyzing the VeroClear material is approximately half. This result indicates a likely lower total enthalpy of vaporization for the VeroClear material compared to FDM-processed ABS material. It is also interesting to note that the pyrolysis pressure slope is nearly linear for the ABS specimens, indicating a nearly constant rate of pyrolysis. For the VeroClear specimen, all of the curves exhibit a significant change of slope after approximately 2-3 seconds, indicating a significant drop in pyrolysis rate as the material heats up. The VeroClear specimens also exhibited wide variability in the pyrolysis rate. Although the WPC specimen shows a good burn-to-burn consistency, this material exhibits by far the smallest arc-pyrolysis rate.

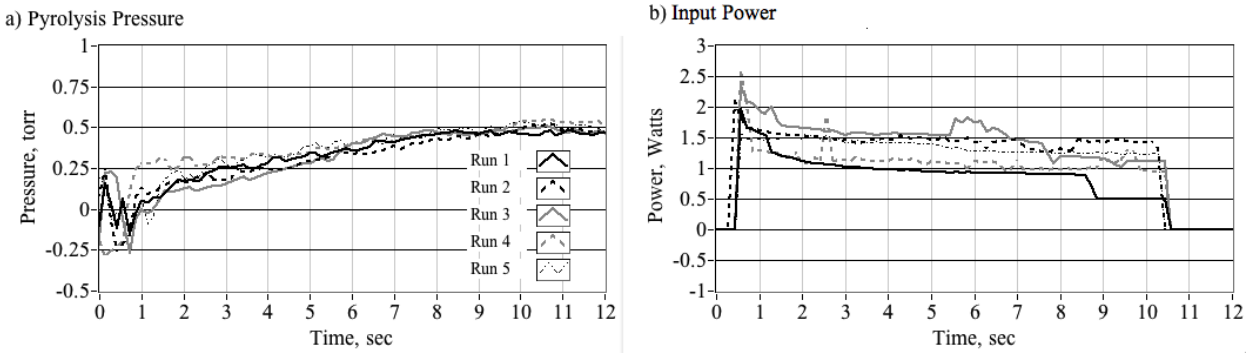

Figure 8. Typical Arc-Pyrolysis Test Results for High-Density ABS Test Specimen.

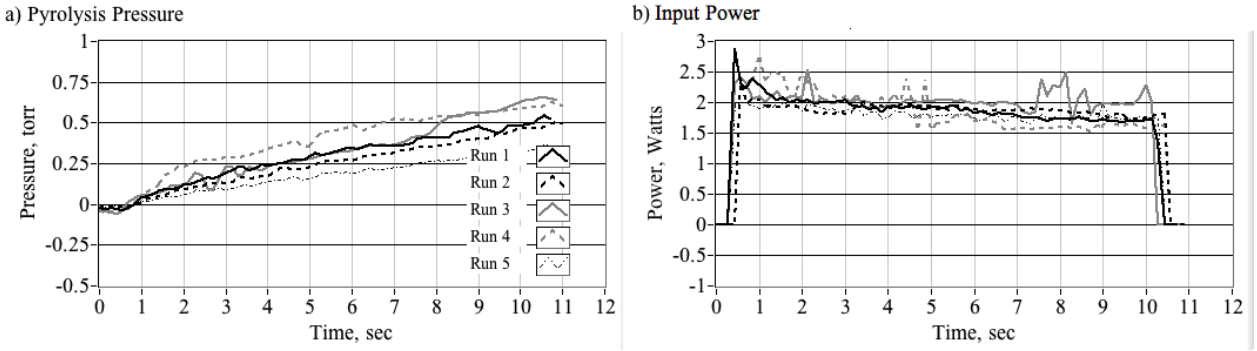

Figure 9. Typical Arc-Pyrolysis Test Results for Low-Density ABS Test Specimen.

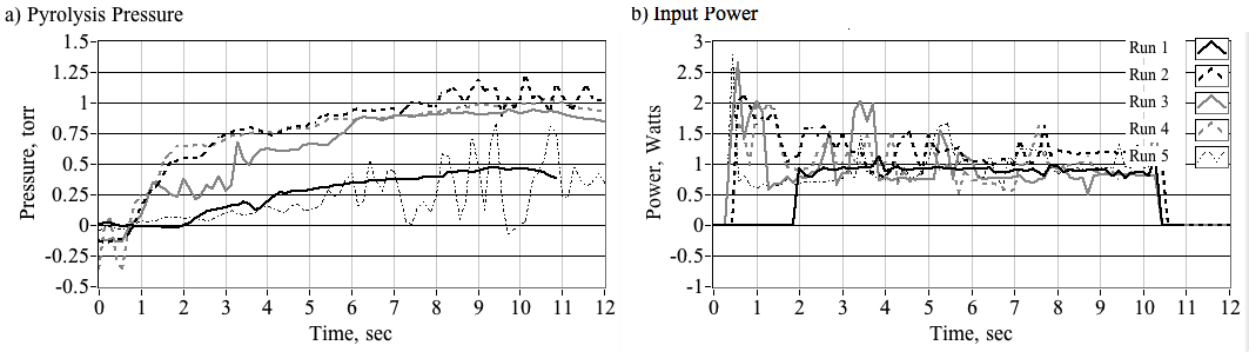

Figure 10. Typical Arc-Pyrolysis Test Results for VeroClear Test Specimen.

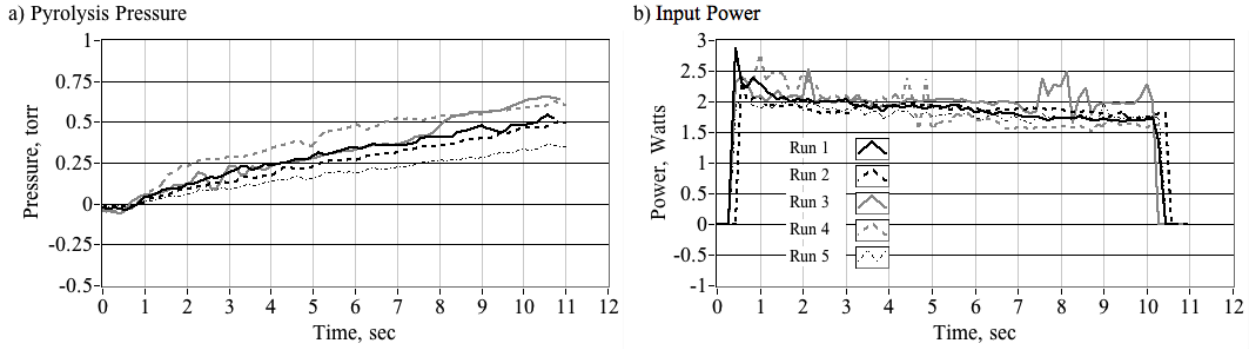

Figure 11. Typical Arc-Pyrolysis Test Results for WPC Test Specimen.

The bar graphs plotted in Figure 12 summarize the pyrolysis tests results for each of the 4 down-selected fuel grain materials. Figure 12(a) compares the mean pyrolysis rates and Figure 12(b) compares the mean input power dissipation in the grain material. The pyrolysis rate was calculated by curve fitting pressure curve to calculate the slope, and then averaging that result over the number of trial runs. The error bars indicate the 95% confidence interval based on the student-t distribution for the appropriate degrees of freedom. Clearly, the low-density ABS and VeroClear stand out as the best potential ignitor grain section materials. The error bars represent 95% confidence levels derived from the sample standard-deviations of the data sets, and using the student-t distribution with 4 degrees of freedom. [20]

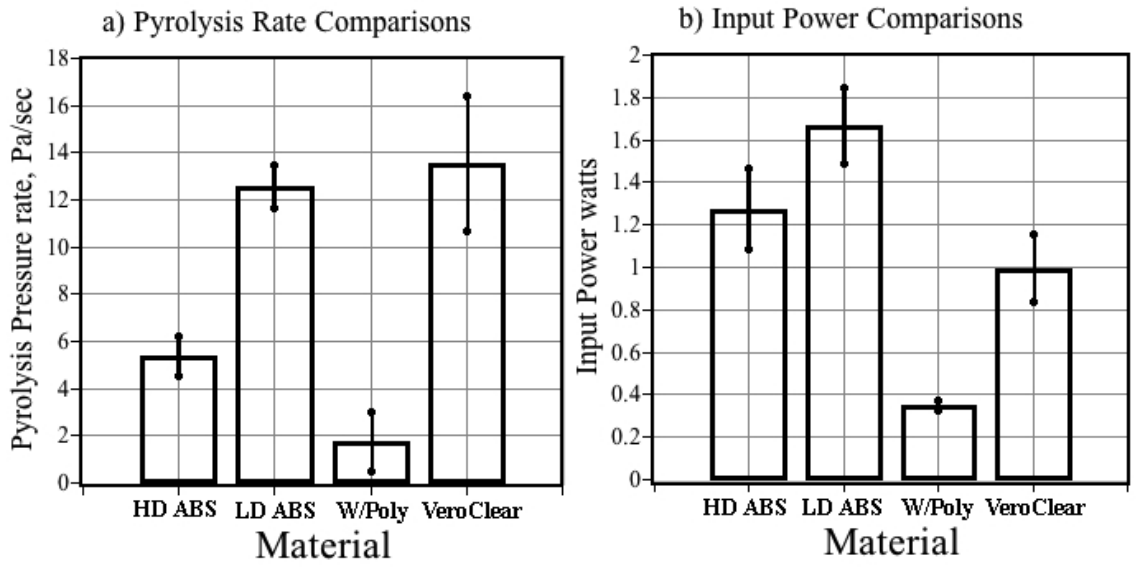

Figure 12. Arc-Pyrolysis Pressure Rate and Power Dissipation Comparison of the 4-Downselected Additively-Manufactured Fuel Materials.

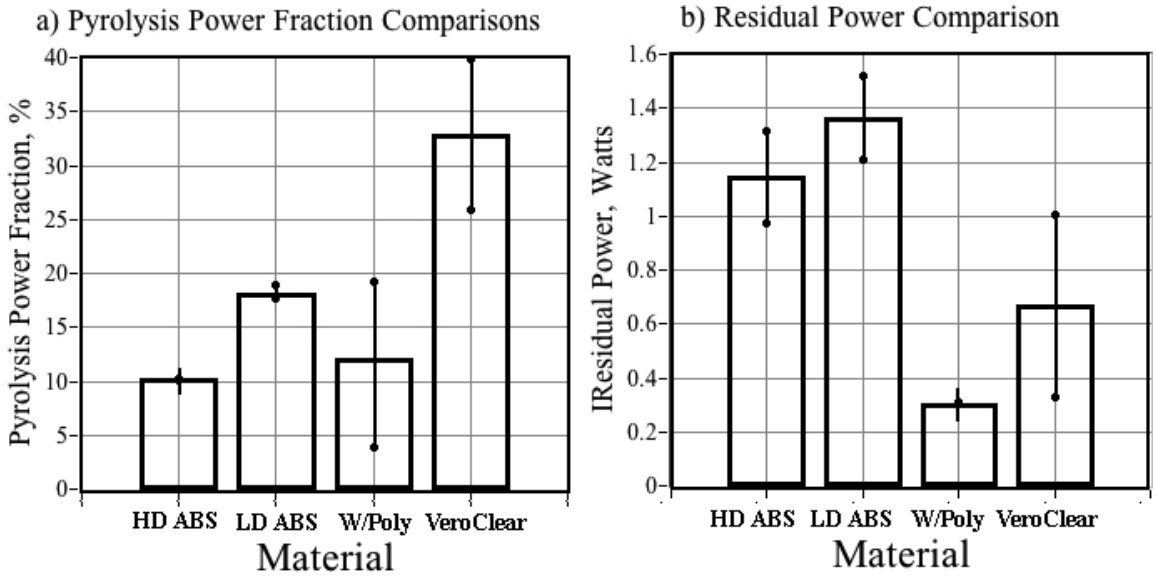

Figure 13. Required Power Fraction for Fuel Pyrolysis and Residual Power After Pyrolysis the 4-Downselected Additively-Manufactured Fuel Materials.

6. Efficiency of the Pyrolysis Process

The data presented by Figure 12 can be used to estimate the fraction of the input power required to pyrolyze the fuel material, and the residual fraction used to initiate ignition in the presence of the oxidizing agent. Assuming a

constant mean gas temperature within the test chamber[11], the mass-flow of the pyrolyzed fuel material is calculated by

$$\dot{m} = \dot{\rho} \cdot V_{ol} = \frac{\dot{p}}{R_g \cdot T} \cdot V_{ol} \ . \tag{1}$$

The energy required to pyrolyze the fuel material is estimated as

$$E = h_v \ \ m = h_v \quad \frac{p}{R_g \ \ T} \quad V_{ol} \ . \tag{2}$$

The fraction of input power required to pyrolyze sufficient fuel to produce the observed mass flow rate is

$$\frac{\dot{E}}{P_{dissipated}} = \frac{h_v \cdot \left(\frac{\dot{p}}{R_g \cdot T} \right) \cdot V_{ol}}{\left(I \cdot V \right)_{HVPS}} . \tag{3}$$

In Equations (1) and (2) p is the pyrolysis pressure rate taken from Figure 12a for high-density ABS, R_g is the gas constant for the pyrolized fuel products as estimated by the NASA equilibrium gas-chemistry code *Chemical Equilibrium with Applications* CEA [22], T is an assumed mean gas temperature range in the cylinder -- approximately *300 K*, V_{ol} is the entrapped internal volume – approximately 100 cm^3, h_v is the enthalpy of gasification – 3.0 MJ/kg (Ref. 21). The parameter $(I \bullet V)_{HVPS}$ is the power output from the high voltage power supply (HVPS) as plotted on Fig 12b, calculated as the product of the sensed output voltage and current.

Figure 13 compares the calculations for the input power fraction required to pyrolyze the fuel material, and also calculates the residual power calculated as the difference between the input power and the power required to pyrolyze the fuel. Previously, Whitmore, and Wilson [23], [24] measured the total enthalpy of gasification of 3-D printed ABS as *3.0 MJ/kg,* and Stoliarov and Waters[25] measured the total enthalpy of gasification of polycarbonate as *1.74 MJ/kg*. The precise chemical formulation of VeroClear is unknown to the authors; however, since

[11] Due to the very low mass flow generated during these tests, and the relatively larger mass of the test chamber, the constant temperature assumption is reasonable here, and was verified by inserting a thermocouple probe into the test chamber during initial pyrolysis testing.

VeroClear is designed as a printable replacement for transparent thermoplastics like PMMA (polymethlymethlyacrylate) acrylic, the PMMA enthalpy of vaporization *1.63 MJ/kg*, was used as a placeholder for this calculation. [26] To account for the uncertainty of this replacement value a variability of $\pm$25% in h_v was used for the VeroClear power dissipation calculation. For the other material the value of h_v was assumed to be deterministic. The significantly larger error bars observed on the VeroClear charts of Figure 13 reflect this result.

Clearly, both the high and low density ABS fuel materials exhibit the most efficient pyrolysis behavior with more than 1-watt of input power "left over" after the fuel has been pyrolyzed. This residual power is available to initiate combustion. Although the VeroClear exhibits a higher pyrolysis rate than either of the ABS specimens, it also has a significantly lower power residual, leaving less energy available to initiate combustion.

7. Arc-Ignition and Burn Tests.

Finally, each of the 4 down-selected fuel grain specimens were inserted into the "Little Joe" thrust chamber depicted in Figure 2 and burned as hybrid fuel materials. A graphite spacer was inserted to adapt for the shorter length of the fuel grain segments evaluated during this series of tests. Figure 2 shows this spacer. Figure 14a shows the oxidizer flow path piping and instrumentation diagram (P&ID), and Figure 14b presents the ignition system electronics schematic. Gaseous oxygen is fed into the top of the motor cap, and manually set regulator and an electronic run valve manage the oxidizer flow control. A separate electronic circuit provides the ignition spark. A laptop computer manages the motor fire-control operations remotely via an amplified USU extension cable.

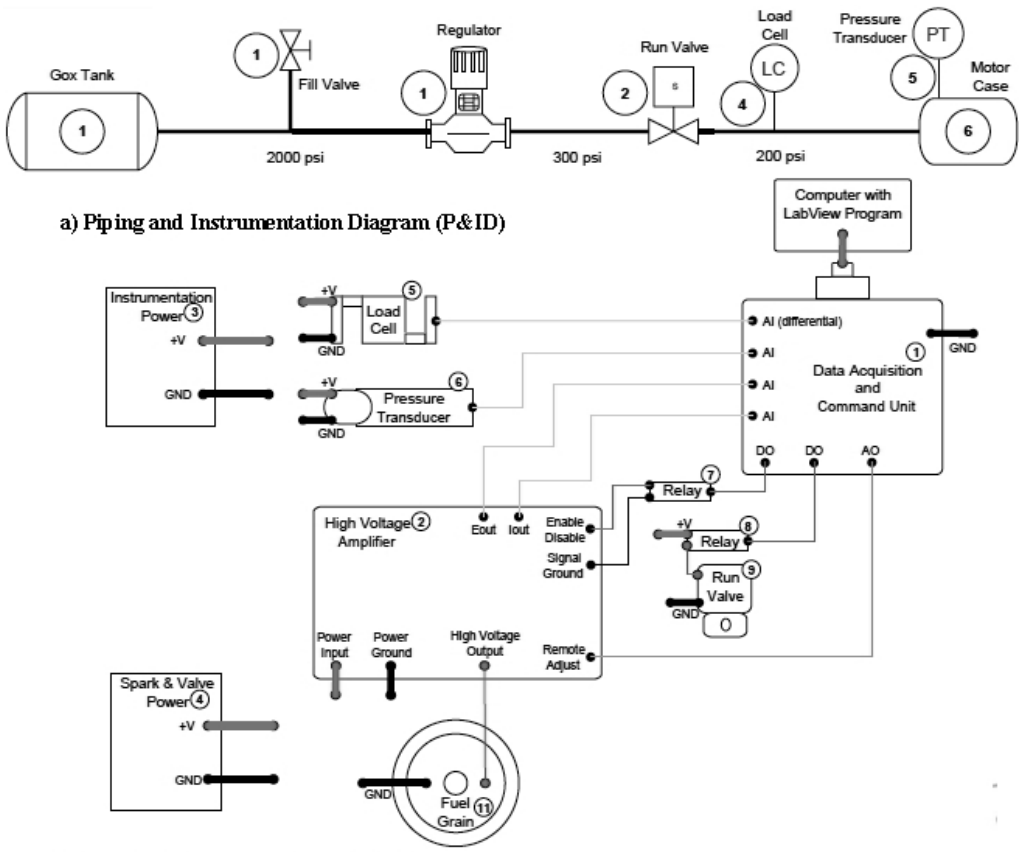

Figure 14. Functional Schematics of "Little Joe" Test Hardware.

Test measurements included combustion chamber pressure, oxidizer mass flow, and thrust. Consumed fuel mass was calculated using pre- and post-test mass measurements. Gaseous oxygen was used as the oxidizer for these tests. The oxidizer mass flow was calculated using a calibrated Venturi flow meter inserted into the GOX flow path. The electronics of the spark-ignition system depicted by Figure 14b was significantly upgraded from the original Little-Joe test apparatus. (Ref. 11) The injector and nozzle geometries remained the same using the coaxial injector with a discharge area of approximately 0.10 cm^2, and a nozzle throat area of approximately 0.28 cm^2.

Because the main objective of this test series was to evaluate the relative ignitability and combustion sustainability with the different fuel materials, the test motor employed only a sonic nozzle in order to simplify the construction; thus, the measured specific impulse has little practical meaning for these tests. For these comparisons the characteristic velocity c^* and combustion efficiencies η^* will be used as the relative measures of merit. The characteristic velocity is calculated from the test measurements by

$$c^*_{measured} = \frac{P_0 \cdot A^*}{\dot{m}} = \frac{P_0 \cdot A^*}{\dot{m}_{ox} \cdot \left(\frac{O/F + 1}{O/F} \right)} = \left(\frac{O/F}{O/F + 1} \right) \cdot \left(\frac{P_0 \cdot A^*}{\dot{m}_{ox}} \right), \quad (4)$$

and the combustion efficiency is estimated by

$$\eta^* = \frac{c^*_{measured}}{c^*_{theory}}, \quad (5$$

In Eq. (4) P_0 is the measured combustor chamber pressure, A^* is the nozzle throat area, $\dot{m}_{ox}$ is the oxidizer mass flow, and *O*/F is the oxidizer-to-fuel ratio. The NASA chemical equilibrium combustion program CEA [23] was used to calculate the theoretical values for c^* based on the mean O/F ratio and chamber pressure. The mean *O/F* ratio was calculated post-test by measuring the consumed fuel and dividing by the total burn time to calculate the mean fuel massflow rate. The oxidizer mass flow rate was measured in real time during the burn tests using the in-line Venturi flow meter. Dividing the measured oxidizer massflow by the mean fuel massflow rate consumption gives the mean O/F value for the burn.

For each test specimen the evaluation motor was commanded to perform 3 consecutive 1-second burns, followed a two-second wait between each burn. Each set of pulse firings was performed twice to ensure run-to-run consistency. Spark was initiated 500 ms before and continued for 500 ms after opening of the GOX run valve. Tests were performed at very low chamber pressures in order to evaluate ignition capabilities under near worst-case conditions. Figure 16 compares these test results for each of the 4-downselected materials. Figures 15(a) -15(c) plots the resulting chamber pressure, oxidizer mass flow, and thrust time histories. Figs. 15(d) - 15(f) plots the input power to the fuel grain, the calculated characteristic velocity *c** based on Eq. (4), and the calculated combustion efficiency based on Eq. (5).

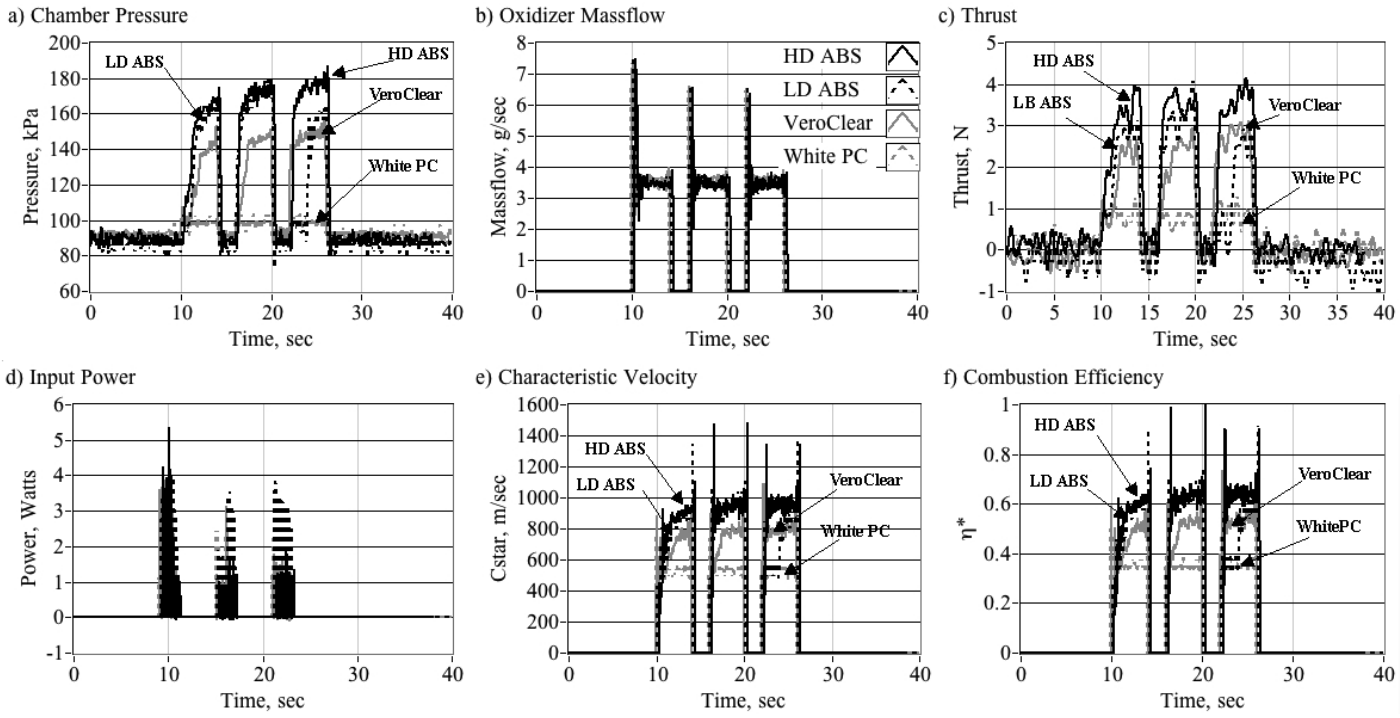

Figure 15: Low Chamber Pressure Hot-Fire Tests Comparisons for the Down-selected Materials.

Only the first three test specimens – 1) high and 2) low density ABS and 3) VeroClear – successfully ignited. For each of these tests the exhaust flame plume was clearly visible, and substantial chamber pressure jumps occurred. The WPC specimen did not ignite in spite of multiple-trials. The small rise in chamber pressure for the WPC trace is only due to the oxidizer massflow. The high- and low-density ABS specimens exhibit nearly identical results. The small latent start for pulse 3 of the low-density ABS is likely due to a surface char build-up that covered the electrodes. Surface arcing and fuel pyrolysis does not typically occur until this char layer burns away. The VeroClear material exhibited significantly less gas production, and the c^* and combustion efficiency η^*, are between 35-40% lower than for the ABS specimens. This result suggests that VeroClear is a lower-performing hydrocarbon when compared to ABS. The low combustion efficiencies for all of the test specimens likely result from the low chamber pressures for these tests, approximately 220 kPa (32 psia). The authors acknowledge that these chamber pressures are significantly lower than the typical levels that occur in a hybrid rocket. However, these pressure levels represent the "ragged edge" of oxidizer concentration that will allow combustion and are considered to be provide a worst-case evaluation of the igntior system effectiveness.

In order to investigate whether the alternative materials – *VeroClear and WPC* -- would perform better under a 25% higher chamber pressure that is more typically a hybrid rocket system, follow on test was performed with 50% higher injector feed pressure. Figure 16 shows these results. Here the VeroClear specimen ignites with slightly less latency than exhibited in Figure 15, and produces a significantly higher chamber pressure. The result is a marginal ~ 10% increase in both c^* and η^*. As with the earlier tests the WPC specimen did not light, and the "bump" in chamber pressure is entirely due to oxidizer inflow. Because the motor did not light, c^* remain largely unchanged.

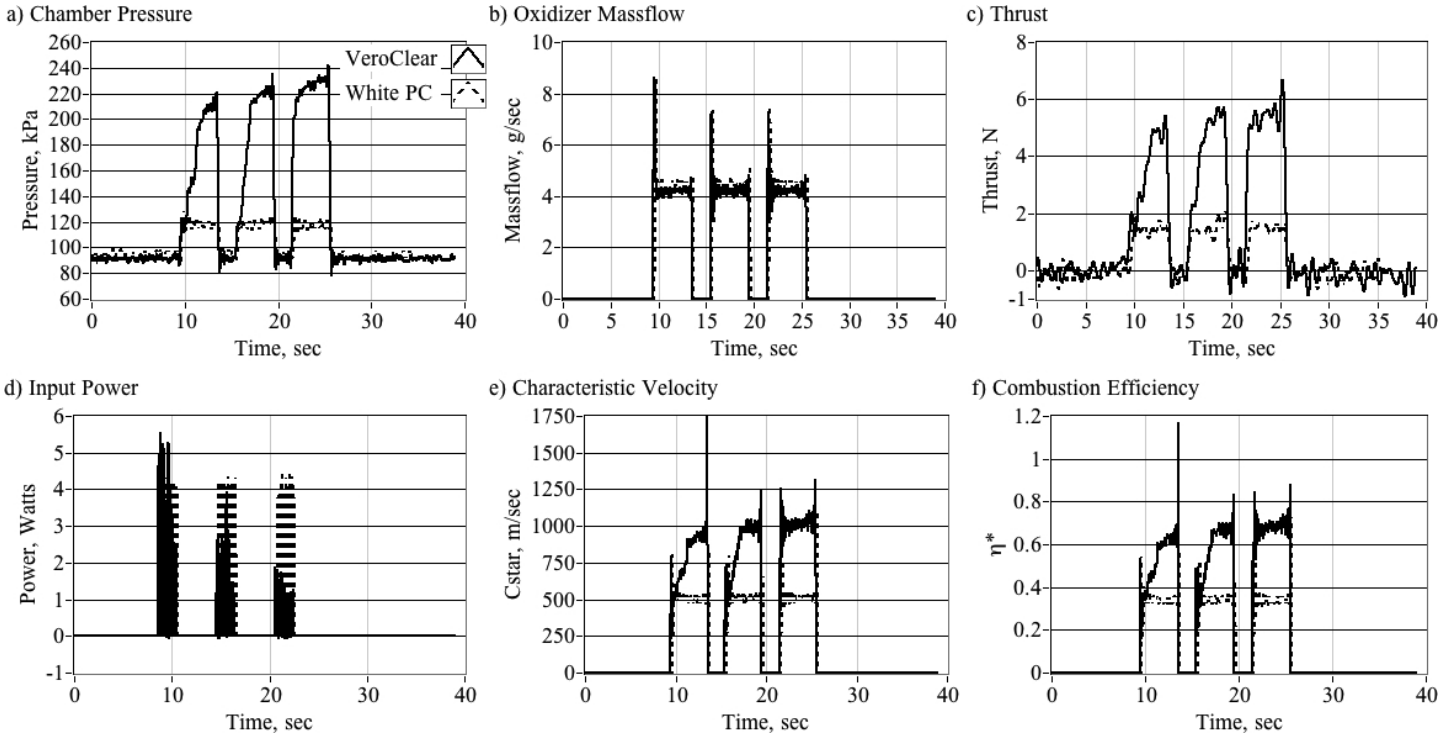

Figure 1**6**: Hot-Fire Results for the VeroClear and WPC at Higher Chamber Pressure.

IV. Conclusion.

The study has investigated commercially-available 3-D printing materials and manufacturing processes to search for equivalent or possibly superior alternatives to FDM-processed ABS as a material for a hybrid rocket featuring an arc-ignition system. Clearly, engineering a printable plastic that is optimized for propulsion applications is a challenging task. Most current printable plastics are engineered for structural/materials and not thermodynamic properties; and as demonstrated by the results of this testing campaign, are unsuitable for propulsion applications. Because the manufacturers hold the precise chemical formulation of their printable plastic as confidential, this test

series did not try to engineer the fuel material that were tested; instead, these tests attempted only to identify which commonly available materials produced the best overall properties for propulsion applications. The test specimens evaluated include photopolymers processed using stereo-lithography (PolyJet) printing, and thermoplastic material printed using fused deposition modeling (FDM). Comparison metrics include general arc-ability, pyrolysis rate, dissipated power, "burnability" at low chamber pressures in a lab-scale hybrid rocket motor, characteristic velocity, and combustion efficiency.

Initially, a set of 8 “printable” polymers was evaluated for minimum spark-ignition capability. With a freshly manufactured grain the material impedance is very high, and the arc generally jumps the air gap between the electrodes. Coating the desired arc path with carbon black and arcing initially sets the fuel material. This action provided a positive path along the material for the spark, and helped to initiate joule heating and pyrolysis of the fuel materials. Once the grain material is “set,” sufficient fuel material has been pyrolyzed to form a slightly conductive char-path along the material surface. This conductive path still possesses impedances typically greater than 10 kΩ; but lower than the air-gap impedance.

Only 4 materials, 1) *High- and 2) Low-density ABS, 3) VeroClear, and 4)* white polycarbonate were found to possess effective “sparking” properties, and were carried forward for arc-pyrolysis measurement. The pyrolysis tests evaluated the rate of hydrocarbon gas generation and required power input levels when the system is subjected to an inductive spark in a closed chamber. Both the High- and Low-density ABS specimens exhibit similar behaviors, except that the low-density material shows a marginally higher pyrolysis rate. The pyrolysis pressures of the low-density ABS and VeroClear are comparable; however, the power consumed in pyrolyzing the VeroClear material is approximately half. This result indicates a likely lower total enthalpy of vaporization for the VeroClear material compared to FDM-processed ABS material. The 4 "surviving" fuel materials were burned as fuel in a small hybrid rocket demonstrator. In follow-on hot-fire burn tests only high- and low-density printed ABS and VeroClear were effective fuel materials. The white polycarbonate material would not ignite. The high-density ABS exhibited the best overall ignition properties and characteristic velocity.

The arc-ignition technology described in this paper has been developed to a high degree of operational readiness, and has been successfully demonstrated for multiple oxidizers including gaseous oxygen and nitrous oxide. The low required input wattage and relatively low required ignition voltages, suggests that this system can be

scaled to large levels. To date reliable "on-demand" system starts and re-starts have been demonstrated across multiple scales with thrust levels varying from less than 10 N to greater than 900 N. Observed ignition latencies and specific impulse from amongst these motor scales were nearly identical, suggesting a high degree of scalability.

A primary technology maturation milestones currently missing is a comprehensive set of systems tests under vacuum conditions, and only this lack of detailed hard-vacuum test data places the TRL of the end-to-end system at the relatively low estimated level of 4-5. A primary focus of immediate follow-on work will be an assessment of the performance of the system under hard vacuum conditions.

Acknowledgements

The authors of this paper would like to acknowledge Dr. John D. DeSain and Mr. Jerome K. Fuller Aerospace Corporation, El Segundo CA for manufacturing the alternative test specimens evaluated during this campaign. Their extensive manufacturing capability and expertise proved to be a very valuable asset to this project.

References

[1] Anon., " Department of Defense Interface Standard, Electromagnetic Environmental Effects requirements for Systems, MIL-STD-464, http:// www.tscm.com/MIL-STD-464.pdf, [Retrieved 8 October 2012].

[2] Bonanos, A. M., Schetz, J. A., O'Brien, W. F., and Goyne, C. P., "Dual-Mode Combustion Experiments with an Integrated Aeroramp-Injector/Plasma-Torch Ignitor", Journal of Propulsion and Power, Vol. 24, No. 2, March-April, 2008, pp. 267-273.

[3] Hulka, J., Forde, J., and Werling, R., "Modification and Verification Testing of a Russian NK-33 Rocket Engine for Reusable and Restartable Applications," AIAA 98- 3361, 1998.

[4] Seamans, T. F., Vanpee, M., and Agosta, V. D., "Development of a Fundamental Model of Hypergolic Ignition in Space-Ambient Engines," AIAA Journal , Vol. 5, No. 1, 1967.

[5] Zakirov, V.A., Lawrence,T. J., Sellers, J. J., and Sweeting, M. N., "Nitrous Oxide as a Rocket Propellant for Small Satellites", Proceedings of the 5th International Symposium on Small Satellite Systems and Services, France, 19-23, June 2000.

[6] Zakirov, V., Sweeting, M., Goeman, V., and Lawrence, T., "Surrey Research on Nitrous Oxide Catalytic Decomposition for Space Applications," SSC00-XI-6, *14th AIAA/USU Conference on Small Satellites, Logan UT, 21-24 August 2000.*

[7] Zakirov, V., Richardson, G., and Sweeting, M., "Surrey Research Update on Nitrous Oxide Catalytic Decomposition for Space Applications," AIAA-2001-3922, 37th AIAA/ASME/SAW/ASEE Joint Propulsion Conference, Salt Lake City UT, 8-11 August 2001.

[8] Whitmore, Stephen A., Peterson, Zachary W., and Eilers, Shannon D., "Comparing Hydroxyl Terminated Polybutadiene and Acrylonitrile Butadiene Styrene as Hybrid Rocket Fuels," AIAA J. Propulsion and Power, vol. 29, no. 3, May–June 2013.

[9] Anon., "Dimension 1200es, Durability Meets Affordability," http://www.stratasys.com/3d-printers," [Retrieved 25 December 2013.]

[10] Stephen A. Whitmore. "Additively Manufactured Acrylonitrile-Butadiene-Styrene–Nitrous-Oxide Hybrid Rocket Motor with Electrostatic Igniter", Journal of Propulsion and Power, Vol. 31, No. 4 (2015), pp. 1217-1220. DOI: 10.2514/1.B35681

[11] Stephen A. Whitmore, Nathan R. Inkley, Daniel P. Merkley, and Michael I. Judson. "Development of a Power-Efficient, Restart-Capable Arc Ignitor for Hybrid Rockets", Journal of Propulsion and Power, Vol. 31, No. 6 (2015), pp. 1739-1749. DOI: 10.2514/1.B35595

[12] McCulley, Jonathan, Bath, Andrew. R., Eilers, Shannon D., and Whitmore, Stephen A., "Design and Testing of FDM Manufactured Paraffin-ABS Hybrid Rocket Motors," AIAA 2012-3962, 48th AIAA/ASME/SAE/ASEE Joint Propulsion Conference & Exhibit, Atlanta, Georgia, 30 July - 01 August 2012.

[13] Stephen A. Whitmore, Sean D. Walker, Daniel P. Merkley, and Mansour Sobbi. "High Regression Rate Hybrid Rocket Fuel Grains with Helical Port Structures", Journal of Propulsion and Power, Vol. 31, No. 6 (2015), pp. 1727-1738. DOI: 10.2514/1.B35615

[14] Anon., ABSplus Spec Sheet, http://usglobalimages.stratasys.com/Main/Secure/Material%20Specs%20MS/Fortus-Material-Specs/Fortus-MS-ABSplus-01-13-web.pdf, [Retrieved 25 December 2014].

[16] Anon, "Stratasys, Polyjet_Materials" http://www.stratasys.com/materials/polyjet, [Retrieved 18 June 2015.]

[17]Anon, Stratasys, FDM Thermoplastics," http://www.stratasys.com/materials/fdm, [Retrieved 18 June 2015.]

[18] Anon., "3D Printing With ABS-ESD7," Stratasys.com, http://www.stratasys.com/materials/fdm/abs-esd7, [Retrieved 25 December 2014].

[19] Anon., "High Power 8C-30C Series, Single Output High Voltage DC/DC Modules," UltraVolt, Inc., *http://www.ultravolt.com/uv_docs/HP8C-30CDS.pdf*, [Retrieved 9 October 2012].

[20] Beckwith, T. G., Marangoni, R. D., and Lienhard V, J. H., Mechanical Measurements, 6th Ed., Prentice Hall, 2006, pp.43-73.

[22] McBride, B. S., and Gordon, S., "Computer Program for Calculation of Complex Chemical Equilibrium Compositions and Applications, NASA RP-1311, October 1994.

[23] Whitmore, S. A., Wilson, J. R., Ritter, M. A., and Williams, L. T., "Pyrolysis of Acrylonitrile Butadiene (ABS) Under High Heat Flux Conditions," AIAA-2014-3752, *50th AIAA/ASME/SAE/ASEE Joint Propulsion Conference and Exhibit,* Cleveland Medical Mart & Convention Center, Cleveland OH, 28-30 July 2014.

[24] Whitmore, S. A., Wilson, J. R., Ritter, M. A., and Williams, L. T., "Estimating the Enthalpy of Gasification of Acrylonitrile–Butadiene–Styrene Hybrid Rocket Fuels", Journal of Propulsion and Power, Vol. 31, No. 4 (2015), pp. 1033-1040. DOI: 10.2514/1.B35621

[25] Stoliarov, S. I., and Walters, R. N., " Determination of the Heats of Gasification of Polymers Using Differential Scanning Calorimetry," *Journal of Polymer Degradation and Stability*, Vol. 93, No., 1, 2008, pp. 422-427.

[26] Gann, R., and Friedman R., *"Principles of Fire behavior and Combustion, 4th ed."* Jones and Bartlett Learning, Publishers, Burlington, MA, pp. 142-143. ISBN-13-978-0-7637-5715-5.